

# Shallow Geophysical Techniques to Investigate the Groundwater Table at the Giza Pyramids Area, Giza, Egypt

S. M. Sharafeldin<sup>1,3</sup>, K. S. Essa<sup>1</sup>, M. A. S. Youssef<sup>2\*</sup>, H. Karsli<sup>3</sup>, Z. E. Diab<sup>1</sup>, and N. Sayil<sup>3</sup>

<sup>1</sup>Geophysics Department, Faculty of Science, Cairo University, Giza, P.O.12613, Egypt

<sup>2</sup>Nuclear Materials Authority, P.O. Box 530, Maadi, Cairo, Egypt

<sup>3</sup>Geophysical Engineering Department, KTU, Turkey

\*shokryam@yahoo.com

## ABSTRACT

The near surface groundwater aquifer that threatened the Great Giza Pyramids of Egypt, was investigated using integrated geophysical surveys. Ten Electrical Resistivity Imaging, 26 Shallow Seismic Refraction and 19 Ground Penetrating Radar surveys were conducted in the Giza Pyramids Plateau. Collected data of each method evaluated by the state-of-the-art processing and modeling techniques. A three-layer model depicts the subsurface layers and better delineates the groundwater aquifer and water table elevation. The aquifer layer resistivity and seismic velocity vary between 40-80  $\Omega$ m and 1500-1800 m/s. The average water table elevation is about +15 meters which is safe for Sphinx Statue, and still subjected to potential hazards from Nazlet Elsamman Suburban where a water table elevation attains 17 m. Shallower water table in Valley Temple and Tomb of Queen Khentkawes of low topographic relief represent a sever hazards. It can be concluded that perched ground water table detected in elevated topography to the west and southwest might be due to runoff and capillary seepage.

*Keywords: Giza Pyramids, Groundwater, Electrical Resistivity, Seismic refraction, GPR.*

## I. INDRDUCTION

In recent years, the 4500 years old Giza Great Pyramids (GGP) of Egypt; Cheops (Khufu), Chephren (Khafre), Menkaure and Sphinx statue; threatened from the rising groundwater table resulted from the water leakage of the suburban, irrigation canals and mass urbanization surrounding the GGP. This problem promoted the need to use non-destructive near surface geophysical techniques integrated with available borehole hydrogeological data to investigate and characterize the groundwater occurrences in the GGP. The GGP located in the southwestern part of the Greater Cairo Region (Fig. 1). Geologically, the Giza Pyramids Plateau composes mainly of white limestone, cream and yellow argillaceous limestone and dark grey dolomitic limestone of Middle-Upper Eocene age. The plateau rocks are commonly interbedded with thin marl layers in their upper part, which dips with about 5-10° to the Southeast (SE) direction. Steep escarpments border the plateau to the north and east directions as shown in Fig. 2 (Yehia, 1985; Mahmoud and Hamdan, 2002). Two regional groundwater aquifers underlie the

38 **Sphinx** (Fig. 3), the Quaternary aquifer of the Nile alluvium, consists of graded sand and gravel  
39 with intercalations of clay lenses at different depths exhibit water table at depth ranges between  
40 1.5 to 4 meters **below ground surface (bgs)**. The second aquifer is fissured carbonate aquifer that  
41 covers the area below the Pyramids Plateau and the Sphinx, where water table ranges in depth of  
42 4 – 7 m bgs. The recharge of the aquifer below Sphinx area occurred mainly through water  
43 system leakage, Irrigation and massive urbanization (AECOM, 2010; and El-Arabi et al., 2013).

44 Many geophysical studies carried out in the GGP mostly for archaeological exploration  
45 and investigations (e.g., Dobecki, T. L., 2005; Abbas et al., 2009 and 2012). Geophysical studies  
46 have an effective contribution in characterizing groundwater aquifers especially geoelectrical  
47 resistivity, seismic refraction and ground penetrating radar techniques. Sharafeldin et al. (2017)  
48 studied the occurrence of the ground water table in GGP using combined VES, ERI and GPR to  
49 investigate the groundwater table in the area. The present work implemented an integration of  
50 Electrical Resistivity Imaging (ERI), Shallow Seismic Refraction (SSR), and Ground Penetrating  
51 Radar (GPR) techniques to depict the groundwater table and characterize the aquifer in the Giza  
52 Pyramids area. **The locations of different surveys conducted in the GGP are illustrated in Fig. 4.**

53

## 54 **II. Method**

### 55 **II.1 Electrical Resistivity Imaging (ERI) Surveys**

56 Two-dimensional electrical resistivity imaging (tomography) surveys are usually carried  
57 out, using a multi-electrode system **with, 24 electrodes** or more, connected to a multi-core cable  
58 (Griffiths and King, 1965). Syscal-Pro resistivity meter, IRIS Instruments, France, was deployed  
59 at the site of the GGP using 24 multi-electrode dipole-dipole array configuration with 5m  
60 electrode spacing. The length of spread is 115m for each profile and attains 23.5 m maximum  
61 depth of investigation. Ten ERI profiles were performed to characterize **the resistivity** of  
62 subsurface layers to delineate the groundwater aquifer (Fig. 4). The topographic elevation of  
63 each electrode is considered along ERI profile and **linked** to the Res2Dinv program. The  
64 acquired ERT data were processed using, Prosys II software of IRIS Instruments, to filter and  
65 exterminate bad and noisy data acquired in the field and produced the pseudo resistivity sections.  
66 The **Res2Dinv** software implemented to invert **the** collected data along conducted ERT profiles  
67 (Loke, and Barker, 1996; Loke, 2012). This software works based upon automatically  
68 subdividing the subsurface of desired profile into several rectangular prisms and then applies an  
69 iterative least-squares inversion algorithm for solving a non-linear set of equations to determine  
70 apparent resistivity values of the assumed prisms while decreasing the misfit values between the  
71 predicted and the measured data. Samples of interpreted data are shown in Figures 5 to 10.

## 73 II.2 Shallow Seismic Refraction (SSR)

74 Seismic refraction is widely used in determining the velocity and depth of weathering  
75 layer, static corrections for the deeper reflection data. It is also employed in civil engineering for  
76 the bedrock investigations and large scale building construction. It is also used in groundwater  
77 investigations, detection of fracture zones in hard rocks, examining stratigraphy and  
78 sedimentology, detecting geologic faults, evaluating karst conditions and for hazardous waste  
79 disposal delineation (Steeple, 2005; Stipe, 2015). A refraction technique is widely developed  
80 for characterizing the groundwater table (Grelle and Guadagno, 2009). Particularly, **the**  
81 **unsaturated soil followed by saturated soil can be separated by a refracting interface** (Haeni,  
82 1988). The seismic velocity values for the depth estimation of the groundwater can be used as an  
83 indicator for water saturation. The values of P-wave velocity are not uniquely correlated to the  
84 aquifer layer, but many authors related the P-wave velocities around 1500 m/s to represent a  
85 saturated layer (Grelle and Guadagno, 2009). The tomographic studies view that the water table  
86 corresponds to a P-wave velocity values of 1100 to 1200 m/s (Azaria et al., 2003; Zelt et al.,  
87 2006).

88 Twenty-six SSR profiles were acquired at GGP (Fig. 4). **OYO McSEIS-SX seismograph**  
89 **with 24 geophones and channels**, was deployed in the GGP site to collect the seismic refraction  
90 data with geophone spacing of 5m. **Sledge hammer with 10Kg** and an **iron-steel** plate are used to  
91 generate seismic P-wave. Five shots per spread were gathered, two off-set forward and reverse,  
92 and a split spread shot. The spread length covers 115m. Due to the historical and touristic nature  
93 of the site, a considerable amount of noise is imposing to the recorded data. These noises were  
94 minimized as possible by using the internal frequency domain filter and **vertical** stacking of  
95 several shots during data acquisition. The first arrival times were picked using SeisImager  
96 software version 4.2 of **Geometrics**. Tomographic inversion; generate initial model from the  
97 velocity model obtained by the time-term inversion, then applying the inversion, which  
98 iteratively traces rays through the model with the goal of minimizing the RMS error between the  
99 observed and calculated travel-times curves (Schuster, 1998). SeisImager utilize a least squares  
100 approach for the inversion step (Zhang and Toksoz, 1998; Sheehan et al., 2005; Valenta, 2007).  
101 A three layers model assumed to represent the subsurface succession with the inverted velocities  
102 and thicknesses. The top most layer exhibits a velocity range of 400-900 m/s, and thickness of 2  
103 and 5 meters, is correlated with loose dry sand, fill and debris. The second layer shows a velocity  
104 range between 1200 and 2400 m/s with 10 to 20 m thick. This layer is correlated with wet and  
105 saturated sand and fractured limestone. The third layer shows a higher domain of velocity, where

106 it ranges between 2800 and 3800 m/s, which can be correlated to marly limestone and limestone.  
107 **The calculated arrival time for the resulted model is compared with the measured arrival time**  
108 **and RMS error is calculated and illustrated on modeled seismic profiles.** Samples of interpreted  
109 data are shown in Figures 5 to 10.

### 110 **II.3 Ground Penetrating Radar (GPR) techniques**

111 GPR is a non-invasive **and effective** geophysical technique to visualize the near surface  
112 structure of the shallow subsurface and widely used to solve the environmental and engineering  
113 problems (Jol and Bristow, 2003; Comas et al., 2004; Neal, 2004). GPR is a site-specific  
114 technique that imposed a vital limitation of the quality and resolution of the acquired data  
115 (Daniels, 2004). The GPR surveys were carried out using 100 MHz shielded antenna of MALA  
116 ProEx GPR. **A total of 19 GPR profiles were performed** along selected locations in the study  
117 area (Figure 4). **The GPR profiles range in lengths from 40 to 200 m**, according to the space  
118 availability, with a total GPR surveys of about 2.5 kilometer. Wheel calibration was **carried out**  
119 near the Great Sphinx along 30 m in distance, the velocity used in calibration is 100 m/ $\mu$ s  
120 **resulted from WAAR test using 100 MHz unshielded antenna of Puls-Echo GPR.** Harari (1996)  
121 showed that the groundwater table can be detected easily with a discerning selection of the  
122 antenna frequency and he observed that the lower frequency antenna (e.g.100 MHz) was more  
123 effective for locating the groundwater table depth. Several basic processing techniques can be  
124 applied to GPR raw data starting from DC-shift to migration (Annan, 2005; Benedetto et al.,  
125 2017). All **19 GPR profiles** were processed to delineate subsurface layering and ground water  
126 elevation in the study area. Appropriate processing sequence **for** GPR data was applied to  
127 facilitate interpretation of radargram sections using REFLEXWIN V. 6.0.9 software (Sandmeier,  
128 2012). **Firstly time-zero correction, and then dewow filters to remove DC component and very**  
129 **low frequency components were applied to all GPR data. Then, a band-pass filter was used to**  
130 **improve the visual quality of the GPR data, gain recovery was applied to enhance the appearance**  
131 **of later arrivals because the effect of signal attenuation and geometrical spreading losses**  
132 **(Cassidy, 2009). Running average filters was the last filter applied. Some sections** of interpreted  
133 data are shown in Figures 5 to 10.

### 134 **III. Results and discussion**

135 The integrated interpretation of the SSR, ERI and GPR surveys **supports** a three layers  
136 model assumed to represent the subsurface succession with the inverted velocities, resistivities  
137 and thicknesses. The top most layer exhibits a velocity range of 400-900 m/s and a resistivity  
138 values varies between 10's to 100's Ohm.m and is correlated with **heterogeneous** loose dry fill  
139 and debris of thickness ranges between 2 and 5 meters. The second layer shows a velocity range

140 between 1200 and 2400 m/s and a resistivity values varies between 40 to 80 Ohm.m, this layer is  
141 correlated with wet and saturated sand and fractured limestone and the thickness varies between  
142 10 to 15 meters. The third layer shows a high velocity ranges between 2800 to 3800 m/s and a  
143 resistivity values varies by changing the topographic elevation and marl intercalation in the  
144 limestone layer. GPR data delineated the subsurface succession and accurate detection of the  
145 water table in area near Sphinx, Valley Temple, Mastaba and Tombs. The **interpreted** ground  
146 water table **elevation** ranges between 14-16 meters in these locations. As the ground relief  
147 increases toward the Mankaura Pyramids the water table is deeper and a perched water table  
148 detected in elevations between 22 to 45 meters.

149 Groundwater rise was detected in some locations **which have an** archaeological  
150 importance, these locations are Nazlet El-samman Village, Sphinx, Sphinx Temple, Valley  
151 Temple of Khafre, Central Field of Mastaba and Khafre Cause Way.

152 **a- Nazlet El-samman Village** is a suburban area located outside the core of the  
153 archeological site. **The geophysical surveys SSR-3 & 4 and GPR-2 conducted in the area**  
154 **show a velocities of 1600-1800 m/s and interpreted water table at elevation of 16-17 m.**  
155 **This elevation is fairly matched with a nearest piezometers-6 and 7 in the area where the**  
156 **ground water elevation is 16-17 m. The aquifer in this part is belonging to the Nile**  
157 **Alluvium Aquifer. This shallow water table might rise the water table level below Sphinx**  
158 **area (Fig. 5), causing a sever hazards.**

159 **b- Sphinx, Sphinx Temple, Valley Temple of Khafre, Central Field of Mastaba and**  
160 **Khafre Cause Way**, this is the most important part of the study where the water appear  
161 on the surface at the Valley temple and surrounding area of the Sphinx. The locations of  
162 the surveys were chosen according to the limited space approved by the Pyramid  
163 Archaeological Authority. The locations of the conducted data are shown in (Fig.4).  
164 Survey shows **a** good matching between the different techniques, where the correlation  
165 between different surveys results, revealed that groundwater elevation between 14-15 m.  
166 **The base level elevation of the Sphinx Status is 20 m, and safe water table elevation**  
167 **should be at elevation of 15 or less.** This level is lower than the suburban area of Nazlet  
168 El-samman, which might indicate a recharge of the aquifer below Sphinx and increase  
169 capillary water rise.

170 **Sphinx and Sphinx Temple**, GPR-9, SSR-13 and ERI-1 conducted in front of Sphinx and  
171 Sphinx Temple. The integration of these surveys in front of Sphinx Temple, the  
172 groundwater elevation is about 14.5-15.5 m, as shown in Figure 6.

173 *Valley Temple of Khafre and central field of Mastaba*, GPR profiles 3, 4, 5, 10 and 11;  
174 SSR profiles 5, 6, 7, 8 and 14; and ERI 2. The integration of this surveys in front of  
175 Valley Temple of Khafre and central field of Mastaba, the groundwater elevation is about  
176 14-15 m as shown in Figure 7.

177 *Tomb of queen Khentkawes*, GPR-11; SSR-15; and ERI-3 conducted near the Tomb.  
178 Figure 7 shows the surveys conduct near the site. The integration of this surveys in front  
179 of Valley Tomb of queen Khentkawes, the groundwater elevation is about 14.5-15 m.

180 *Valley Temple of Menkaure*, GPR-12; SSR-16; and ERI-4 conducted near the Temple.  
181 The integration of these surveys in front of Valley Temple of Menkaure, the groundwater  
182 elevation is about 16.5-17 m. GPR profiles might detect the perched ground water table at  
183 shallower depth from ground level (Fig. 8).

184 *Cause way to Menkaure Pyramid*, show high resistivity value near the surface, and water  
185 table located at elevation ranges from 22 to 24 m. *Menkaure Queens Pyramids and*  
186 *Menkaure Quarry*, where the surveys in this part conducted at higher topographic relief,  
187 the correlation of the different techniques revealed that the water table might be  
188 interpreted at elevations 45-58 m. This might detect the perched ground water table at  
189 shallower depth from ground level (Figs. 9 and 10).

190  
191 Table 1, shows a comparison of the ground water table elevation data recorded in  
192 some piezometers illustrated in (Fig 12), installed by Cairo University in Wdi Temple  
193 and Sphinx area (AECOM, 2010), and the interpreted water table elevation resulted from  
194 nearest conducted geophysical surveys. There is a relatively good agreement between the  
195 results and differences might be related to the tolerance in the geophysical data and exact  
196 physical properties surface between the wet and saturated media. Moreover, the pumping  
197 stations discharge might lower the water table in the site.

198  
199 Figure 11 represents a cross-section, using the ERT and GPR data, to illustrate the difference  
200 of groundwater table elevation between the Great Sphinx to the small pyramids of Menkaure that  
201 indicates the increase of groundwater elevation from west to east. As the average water table  
202 elevation to be about 15 m, the water table to the west might be considered as perched water  
203 table due to leakage, surface runoff and capillary and fracture seepage. Figure 12 represents the  
204 compiled groundwater table elevation contour map from the geophysical surveys, overlay the  
205 groundwater table levels measured from some of the piezometers installed by Cairo University  
206 (AECOM 2010). The present geophysical surveys proved that, the pumping system installed by

207 AECOM 2010 lowering the groundwater levels in some piezometer and a need of more pumping  
208 to compensate the recharge of the water leakage resulted from surrounding area of Sphinx.  
209 Figure 13 shows a 3D representation of the groundwater system in Great Giza Pyramids Plateau  
210 and surrounding area.

## 211 **V. Conclusions**

212 The integrated interpretation of ERT, SSR and GPR surveys **was performed** in Great Giza  
213 Pyramids site successfully investigate the groundwater aquifer and water table **elevation** in Great  
214 Giza Pyramid and assist the hazards mitigation. An interpreted model consists of three layers  
215 assumed to depict the subsurface layers and better delineation of the aquifer layer associated with  
216 resistivity range of 40-80  $\Omega\text{m}$  and seismic velocity of 1500-1800 m/s. The average water table  
217 depth is about 15m, which is safe for the Sphinx status where the base foot at elevation of 20 m.  
218 The water table elevation increases in Nazlet Elsamman Village to **16-17m** and **might recharge**  
219 **the aquifer below** Sphinx and Valley Temple which considered a **sever** hazard on the site. Tomb  
220 of Queen Khentkawes threatened by water leakage resulted from vegetation in old cemetery and  
221 nearby football field. A parched groundwater table might exist in elevated area toward west and  
222 southwest. A great care should be taken to the effect of massive urbanization to the west of the  
223 Great Giza Pyramids which might affect the groundwater model of the area. The dewatering  
224 system should be accomplished to avoid such hazards.

225

## 226 **Acknowledgements**

227 Authors would like to thank Prof. Jothiram Vivekanandan, Chief-Executive Editor, Prof. Andrea  
228 Benedetto, the Associate Editor and the reviewer for their constructive comments for improving  
229 our manuscript. **Geophysics Department, Cairo University furnished all possible facilities to**  
230 **conduct the research. IIE-SRF funded the scholarship of S. M Sharafeldin hosted by Geophysical**  
231 **Engineering Department, KTU, Turkey. Supreme Council of Archaeological authority**  
232 **permission to conduct the surveys is highly acknowledged.**

233

234

235

236

237

238

239

240

241

242 **References**

- 243 Abbas, A. M., Atya, M., EL-Emam, A., Ghazala, H., Shabaan, F., Odah, H., El-Kheder, I., and  
244 Lethy, A.: Integrated Geophysical Studies to Image the Remains of Amenemeht- II Pyramid's  
245 Complex in Dahshour Necropolis, Giza, Egypt. NRIAG, 2009.  
246 <https://www.researchgate.net/publication/234180809>.
- 247
- 248 Abbas, A. M., El-sayed, E. A., Shaaban, F. A., and Abdel-Hafez, T.: Uncovering the Pyramids-  
249 Giza Plateau in a Search for Archaeological Relics by Utilizing Ground Penetrating Radar.  
250 Journal of American Science, 8(2), 1-16, 2012.
- 251
- 252 AECOM, ECG, and EDG: Pyramids Plateau Groundwater Lowering Activity. Groundwater  
253 Modeling and Alternatives Evaluation. USAID Contract No EDH-I-00-08-00024-00-Order  
254 No.02, 2010.
- 255
- 256 Annan, A. P., [2005] Ground-penetrating radar. In Near surface geophysics, Butler DK (ed).  
257 Society of exploration geophysicists: Tulsa, Investigations in Geophysics 13, 357-438.
- 258
- 259 Azaria, A., Zelt, C. A., and Levander, A.: High-resolution seismic mapping at a groundwater  
260 contamination site: 3-D travelttime tomography of refraction data. EGS–AGU–EUG joint  
261 Assembly, Abstracts from the meeting held in Nice, 2003.
- 262
- 263 Benedetto, A., Tosti, F., Ciampoli, L. B., and D’Amico, F.: An overview of ground-penetrating  
264 radar signal processing techniques for road inspections. Signal Processing, 132, 201-209, 2017.
- 265
- 266 Cassidy, N. J.: Ground penetrating radar data processing, modelling and analysis. In Ground  
267 penetrating radar: theory and applications, Jol HM (ed). Elsevier:Amsterdam, 141-176, 2009.
- 268
- 269 Comas X., Slater L. and Reeve A.: Geophysical evidence for peat basin morphology and  
270 stratigraphic controls on vegetation observed in a northern peat land. Journal of Hydrology, 295,  
271 173-184, 2004.
- 272
- 273 Daniels, D.J.: Ground penetrating radar (2nd edition). The Institution of Electrical Engineers:  
274 London, 2004.
- 275
- 276 Dobecki, T. L.: Geophysical Exploration at the Giza Plateau, Egypt a Ten-Year Odyssey.  
277 Environmental & Engineering Geophysical Society (EEGS). 18th EEGS Symposium on the  
278 Application of Geophysics to Engineering and Environmental Problems, 2005.
- 279
- 280 El-Arabi, N., Fekri, A., Zaghoul, E. A., Elbeih, S. F., and laake A.: Assessment of  
281 Groundwater Movement at Giza Pyramids Plateau Using GIS Techniques. Journal of Applied  
282 Sciences Research, 9(8), 4711-4722, 2013.
- 283
- 284 Grelle, G. and Guadagno, F. M.: Seismic refraction methodology for groundwater level  
285 determination: “Water seismic index”. Journal of Applied Geophysics 68, 301–320, 2009.
- 286

287 Griffiths D. H. and King R. F.: Applied geophysics for Engineering and geologists, Pergamon  
288 press, Oxford, New York, Toronto, 221p, 1965.  
289

290 Harari, Z.: Ground-penetrating radar (GPR) for imaging stratigraphic features and  
291 groundwater in sand dunes. J. Appl. Geophys., 36, 43–52, 1996.  
292

293 Jol, H. M. and Bristow C. S.: GPR in sediments: advice on data collection, basic processing and  
294 interpretation, a good practice guide. In Ground penetrating radar in sediments, Bristow CS and  
295 Jol HM (ed). Geological Society: London, Special Publication 211; 9- 28, 2003.  
296

297 Loke, M. H., and Barker, R. D.: Rapid least-squares inversion of apparent resistivity pseudo-  
298 sections by a quasi- Newton method. Geophysical Prospecting, 44 (1), 131–152, 1996.  
299

300 Loke M. H.: Tutorial: 2-D and 3-D electrical imaging surveys. Course Notes, 2012.  
301

302 Mahmoud, A. A., and Hamdan, M. A.: On the stratigraphy and lithofacies of the Pleistocene  
303 sediments at Giza pyramidal area, Cairo, Egypt. Sedimentology of Egypt, 10, 145-158, 2002.  
304

305 Neal A.: Ground-penetrating radar and its use in sedimentology: principles, problems and  
306 progress. Earth science reviews, 66, 261-330, 2004.  
307

308 Sandmeier, K. J.: The 2D processing and 2D/3D interpretation software for GPR, reflection  
309 Seismic and refraction seismic. Karlsruhe, Germany. <http://www.sandmeier-geo.de/>, 2012.  
310

311 Schuster, G. T.: Basics of Exploration Seismology and Tomography. Basics of Traveltime  
312 Tomography. Stanford Mathematical Geophysics Summer School Lectures. 1998.  
313 (<http://utam.geophys.utah.edu/stanford/node25.html>).  
314

315 Sharafeldin, M., Essa, K.S. , Sayil, N. , Youssef, M.S., Diab, Z. E., and Karshi, H.:  
316 Geophysical Investigation Of Ground Water Hazards In Giza Pyramids And Sphinx Using  
317 Electrical Resistivity Tomography And Ground Penetrating Radar: A Case Study. Extended  
318 Abstract, 9th Congress of the Balkan Geophysical Society, Antalya, Turkey. DOI: 10.3997/2214-  
319 4609.201702549, 2017.  
320

321 Sheehan, J. R., Doll, W. E., and Mandell, W. A.: An Evaluation of Methods and Available  
322 Software for Seismic Refraction Tomography Analysis. JEEG, 10 (1), 21–34, 2005.  
323

324 Steeples, D. W.: Shallow Seismic Methods. In Y. Rubin, & S. S. Hubbard, Hydrogeophysics (pp:  
325 215-251). Netherlands: Springer, 2005.  
326

327 Stipe, T.: A Hydrogeophysical Investigation of Logan, MT Using Electrical Techniques and  
328 Seismic Refraction Tomography. Degree of Master of Science in Geoscience: Geophysical  
329 Engineering Option. Montana Tech., 2015.  
330

331 Valenta, J., and Dohnal, J.: 3D seismic travel time surveying – a comparison of the time- term  
332 method and tomography (an example from an archaeological site). *Journal of Applied*  
333 *Geophysics*, 63, 46-58, 2007.  
334

335 Yehia A.: Geological structures of the Giza pyramids plateau. Middle East Res. Center, Ain  
336 Shams Univ., Egypt, *Sci. Res. Series*, 5, 100-120, 1985.  
337

338 Zelt, A. C., Azaria, A., and Levander, A.: 3D seismic refraction travel time tomography at a  
339 groundwater contamination site. *Geophysics*, 58(9), 1314–1323, 2006.  
340

341 Zhang, J., and Toksoz, M.: Nonlinear refraction travelttime tomography. *Geophysics*, 63(5),  
342 1726–1737, 1998.  
343  
344  
345  
346  
347  
348  
349  
350  
351  
352  
353  
354  
355  
356  
357  
358  
359  
360  
361  
362  
363  
364  
365  
366  
367  
368  
369  
370  
371  
372  
373

374 Table 1: Average interpreted Groundwater elevations to the nearest 8 piezometers, installed  
 375 piezometers (modified after EACOM 2010)

Piezom. No.	Surveyed Area	Geophysical Data	Piezom.GWT (m)	Interpreted GWT (m)
PZ-6 & 7	Nazlet Elsamam	SSR3 & 4 GPR2, 5	15.9-17.4	16-17
PZ-8	Sphinx Temple	SSR3& 4, GPR2 ,5 ERI1	15.7	14.5-15.5
PZ-11 & 14	Valley Temple	SSR14,GPR10 & ERI2	14.4 – 14.1	14-15
PZ-12, 15 &16	Sphinx	SSR13, GPR9 & ERI1	15.3- 15.6	15-15.5

376

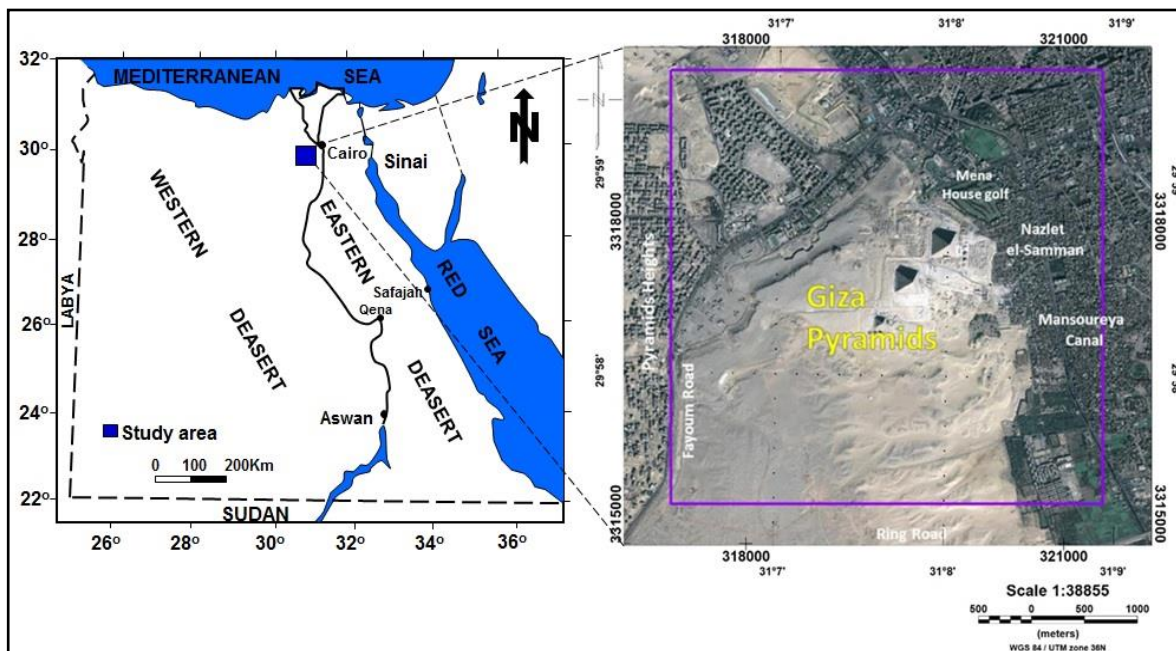


Fig. 1: Location map of the study area of Pyramids Plateau.

377  
 378  
 379  
 380  
 381

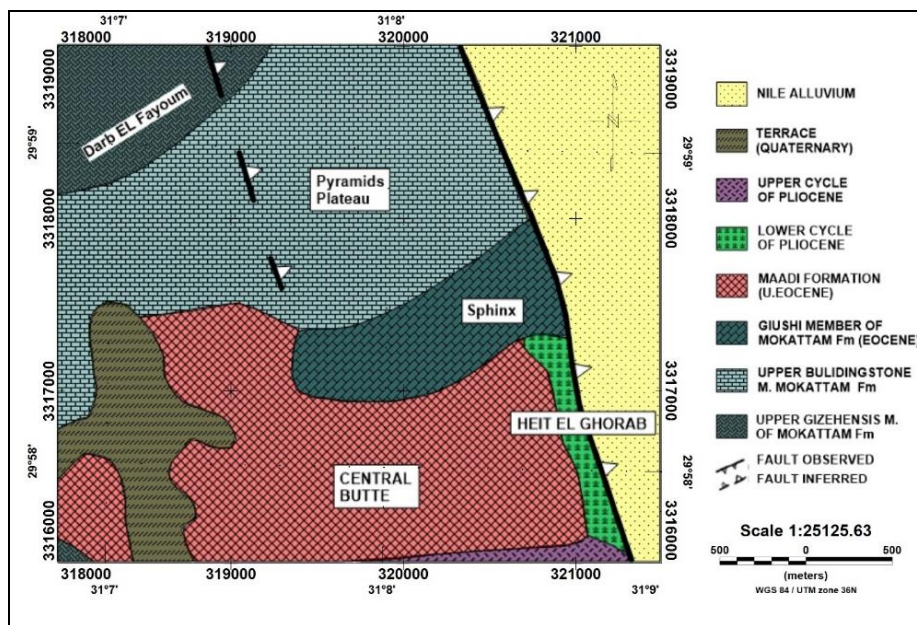


Fig. 2: Geologic map of the Giza Pyramid Plateau, Egypt. (Modified after Yehia, 1985).

382  
 383  
 384  
 385  
 386

387  
 388  
 389  
 390  
 391  
 392  
 393  
 394  
 395  
 396  
 397  
 398  
 399  
 400  
 401  
 402  
 403  
 404  
 405  
 406  
 407  
 408  
 409

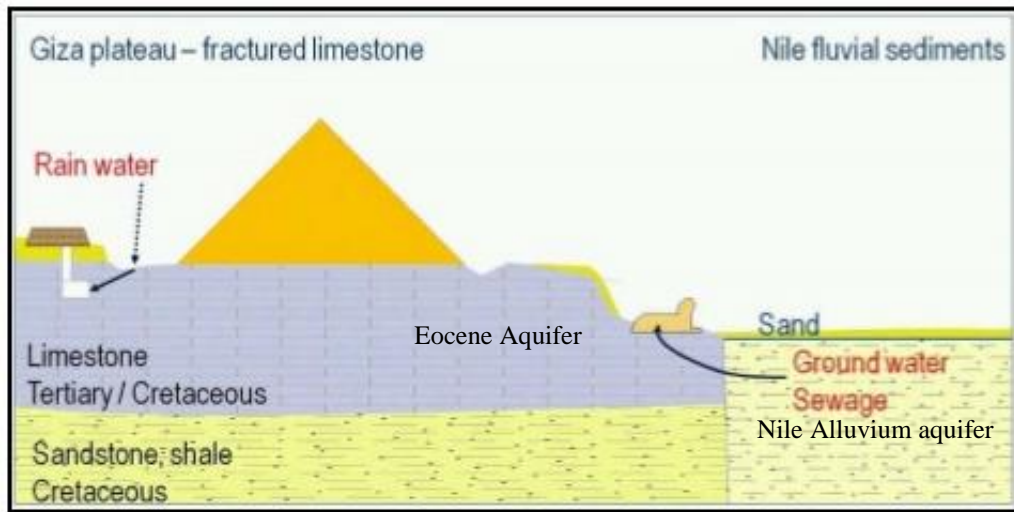
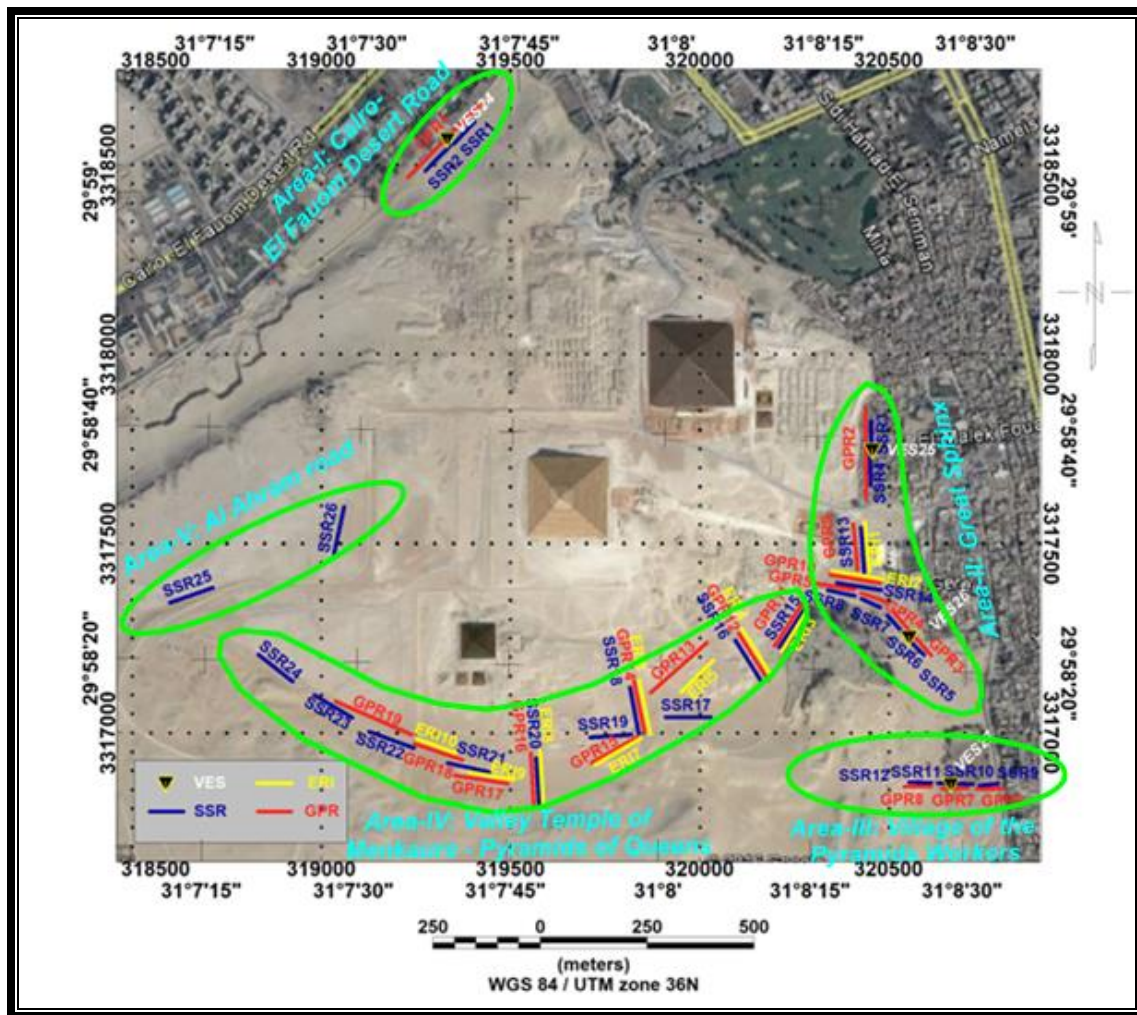
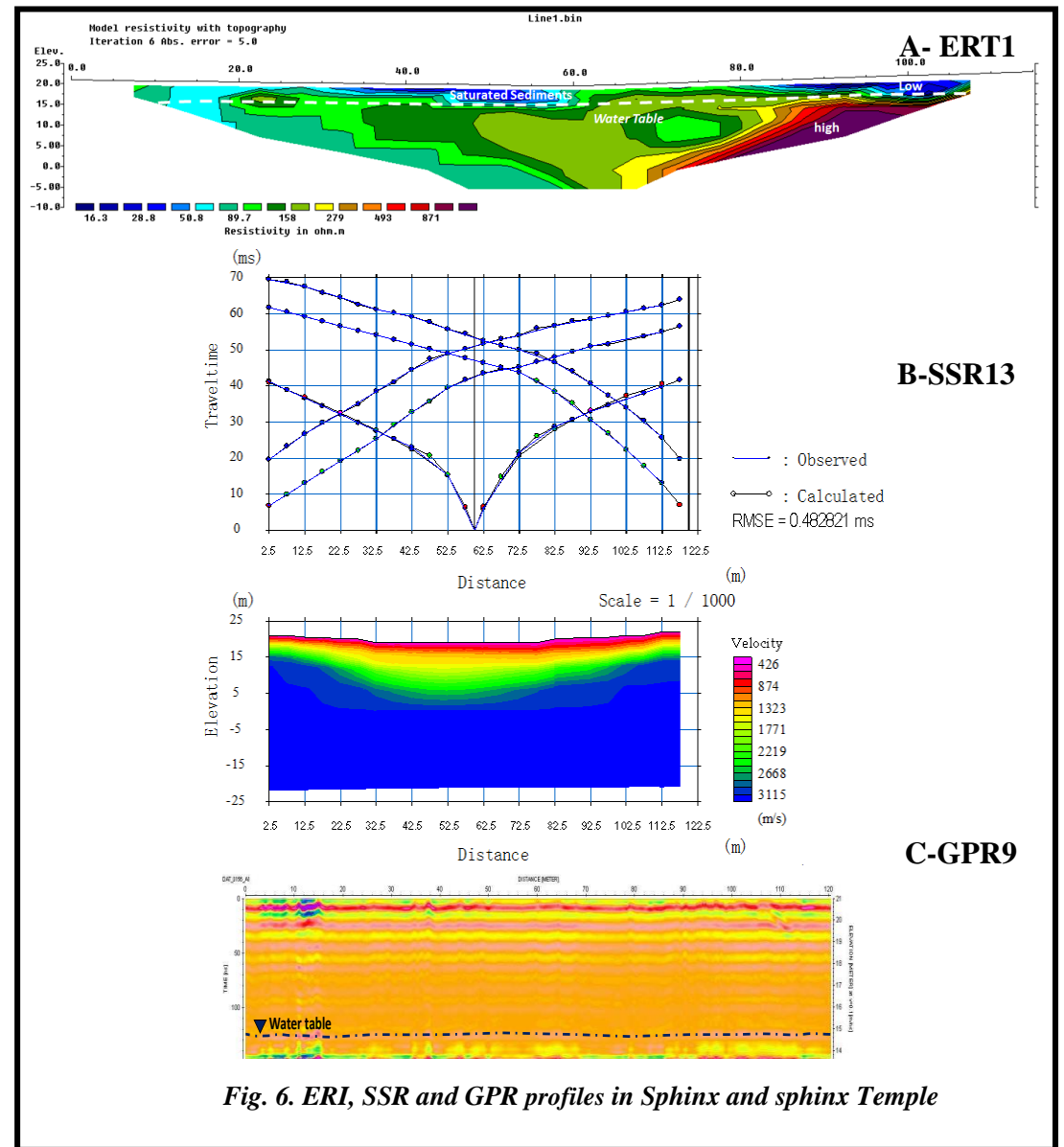
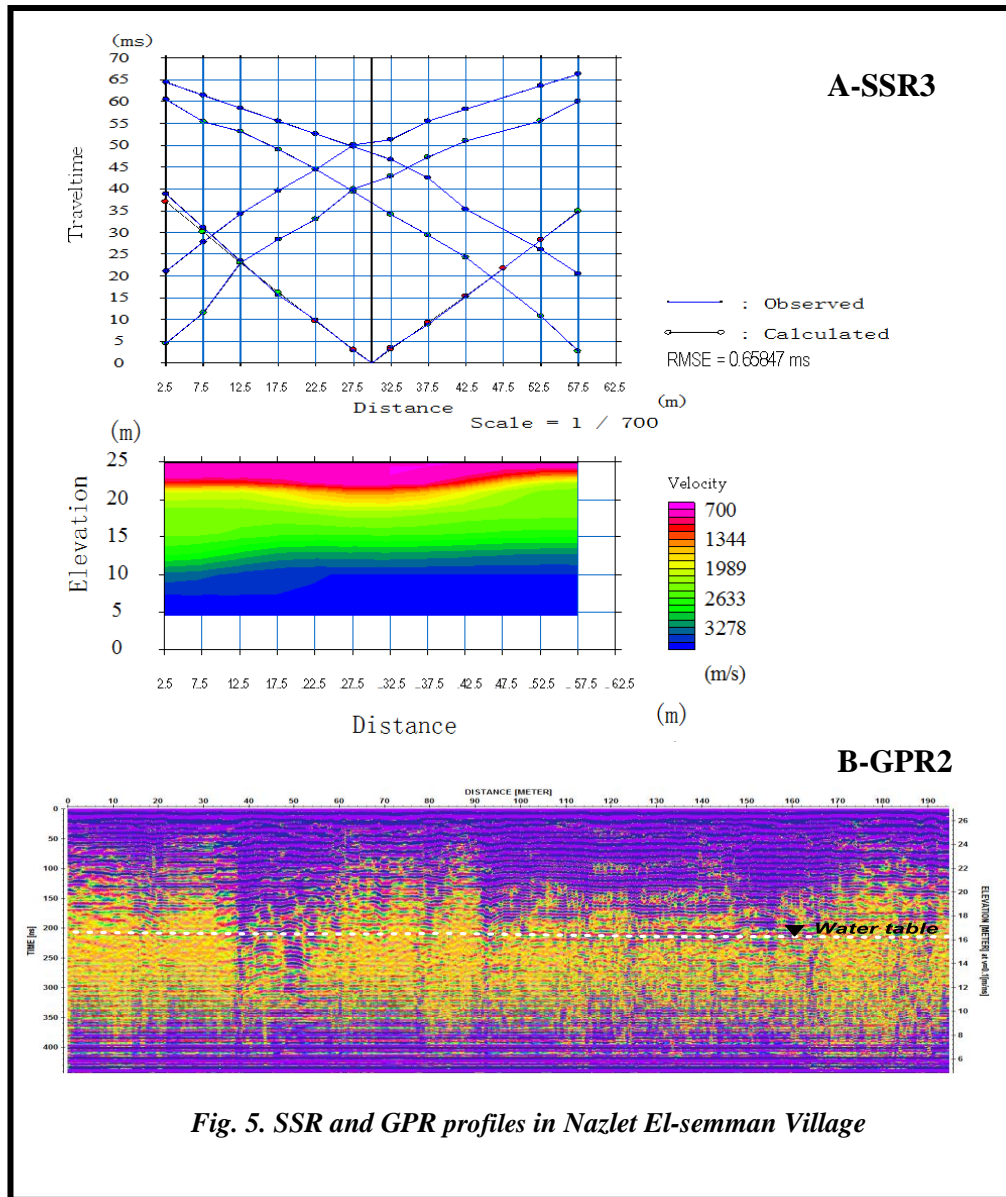


Fig. 3 Ground water aquifers affected the Giza Pyramids Plateau (El-Arabi et al., 2013).



410  
 411

Fig. 4: locations for the profiles and techniques used along the different parts of the Giza Pyramids plateau.



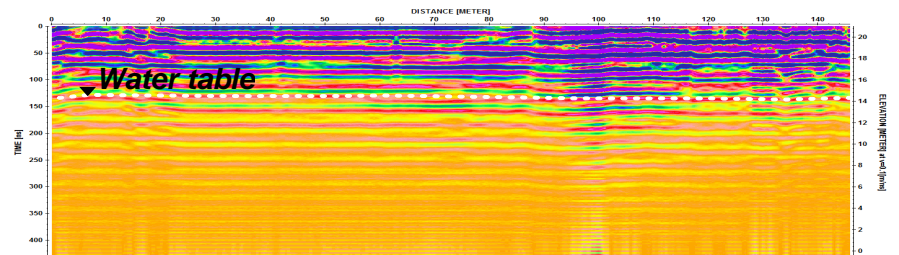
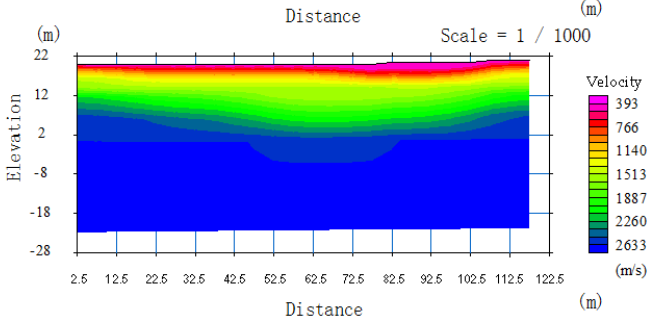
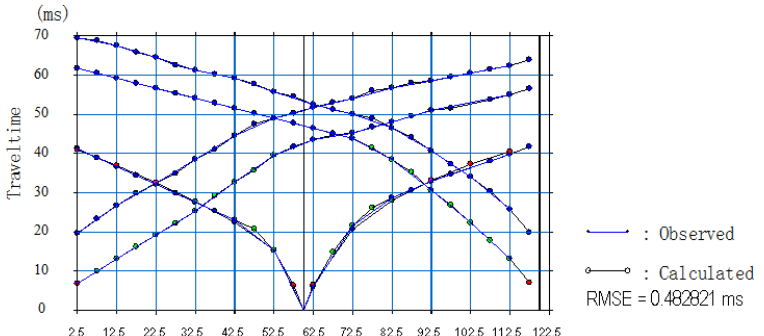
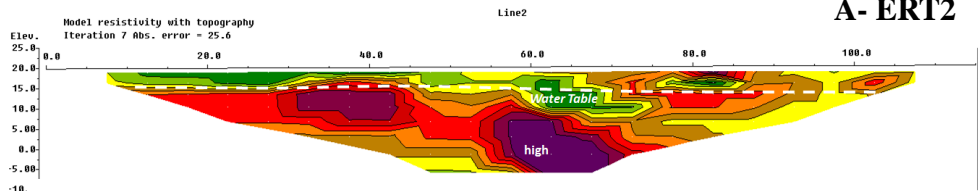


Fig. 7. ERT, SSR and GPR profiles in Valley Temple of Khafre and central field of Mastaba

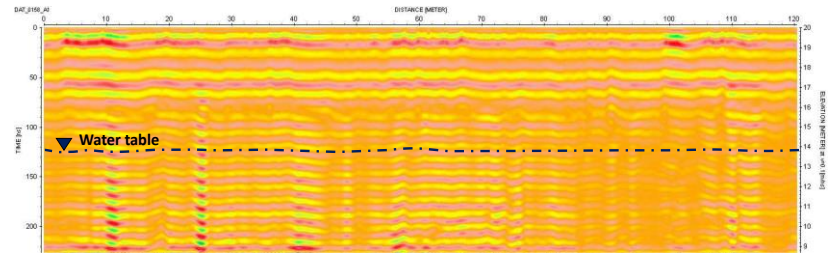
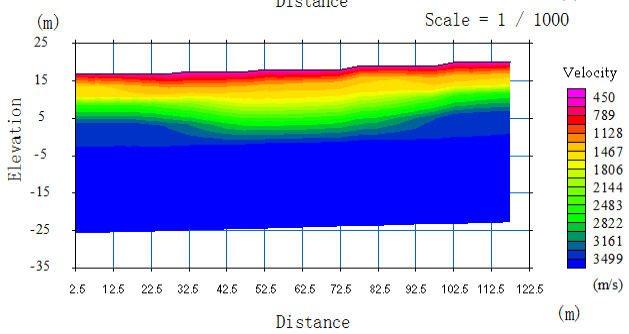
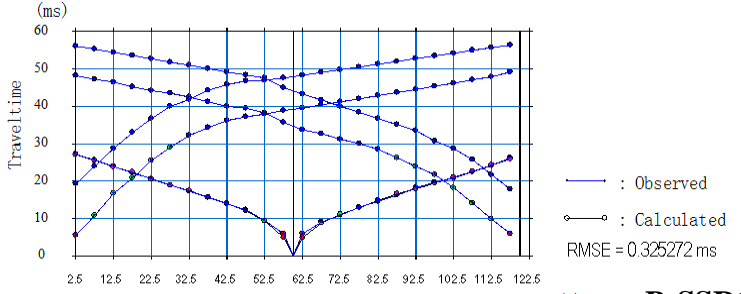
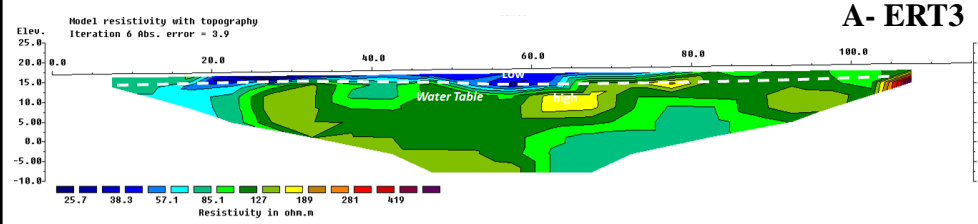


Fig. 8. ERT, SSR and GPR profiles in Tomb of queen Khenkawes

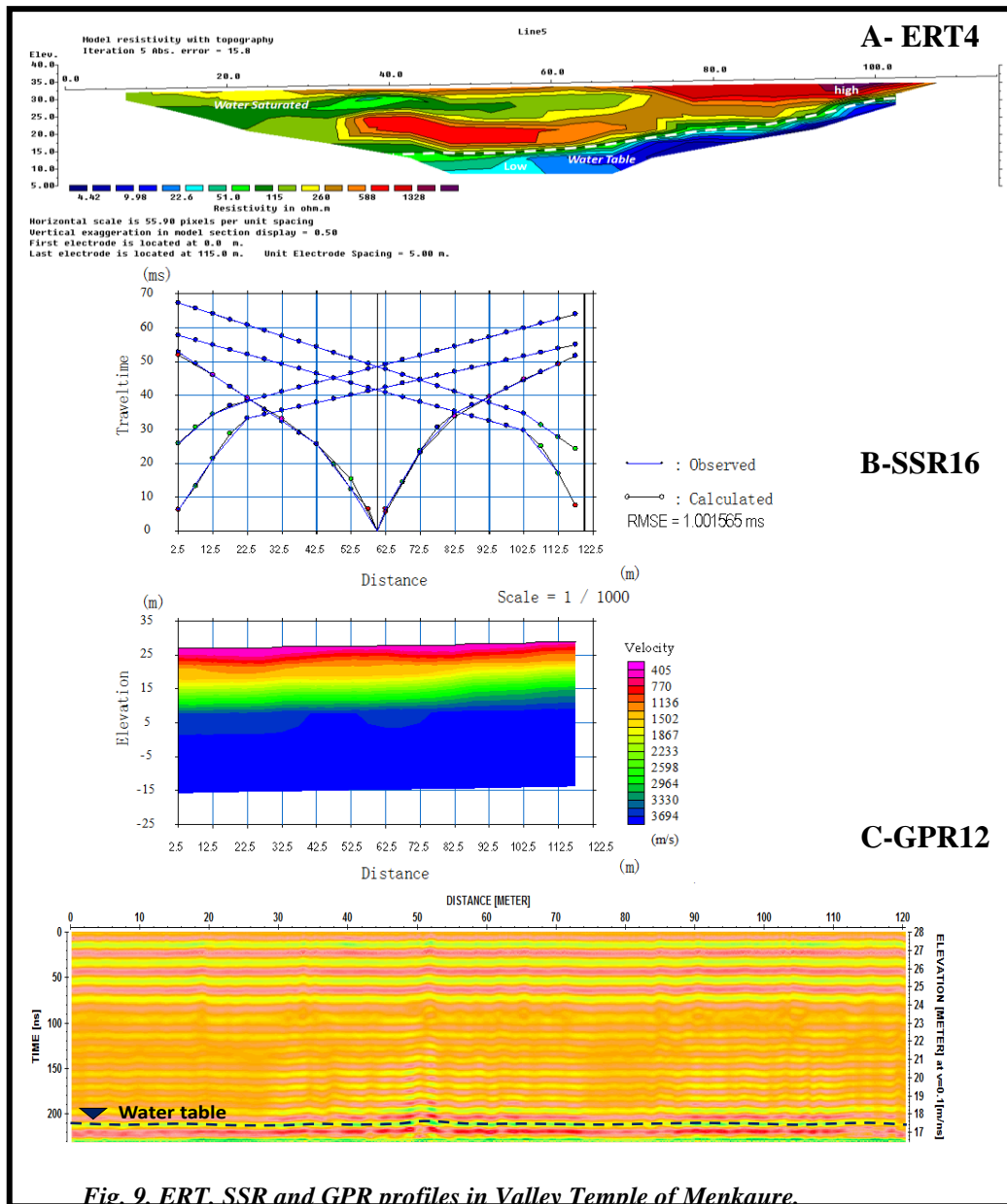


Fig. 9. ERT, SSR and GPR profiles in Valley Temple of Menkaure.

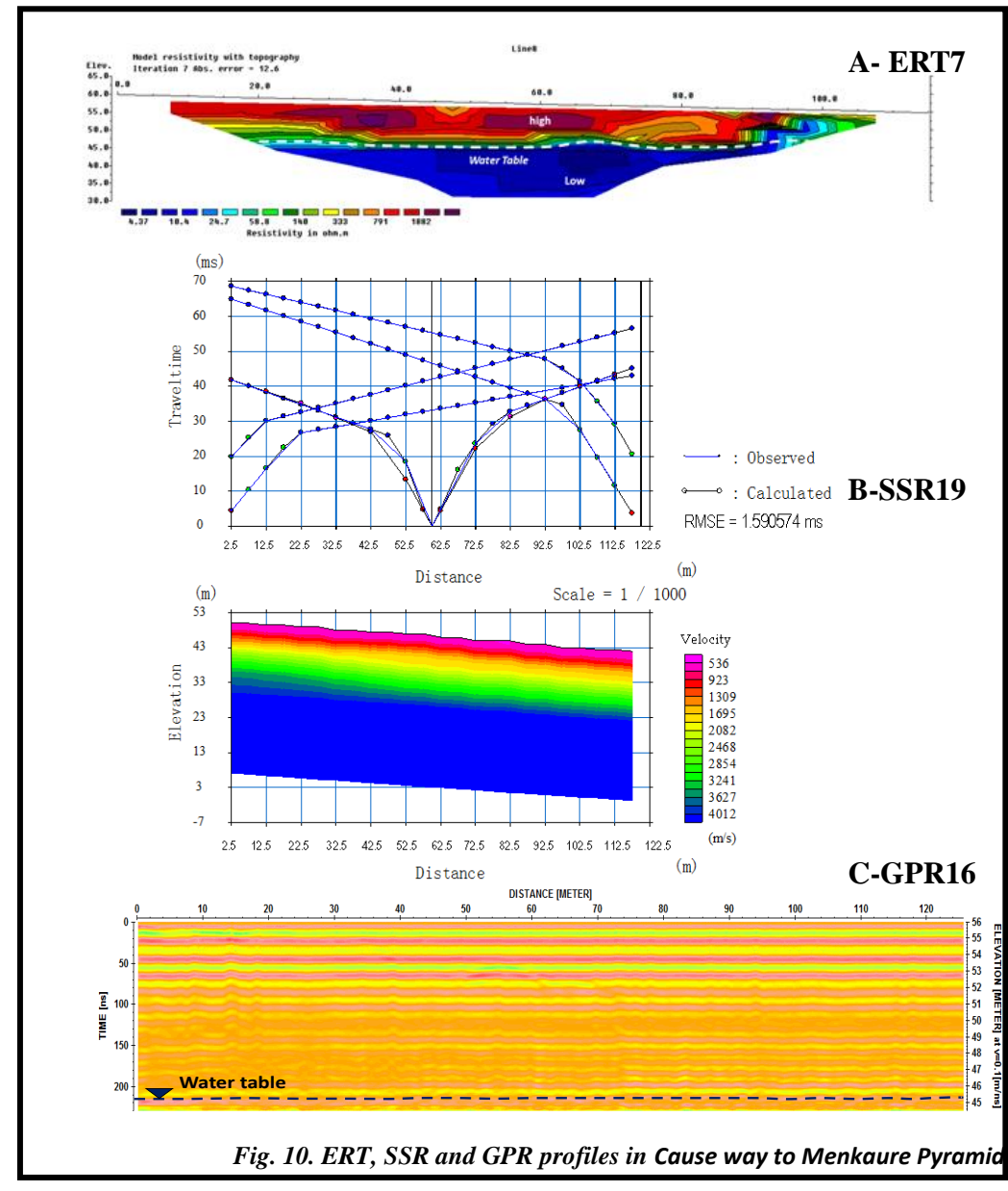
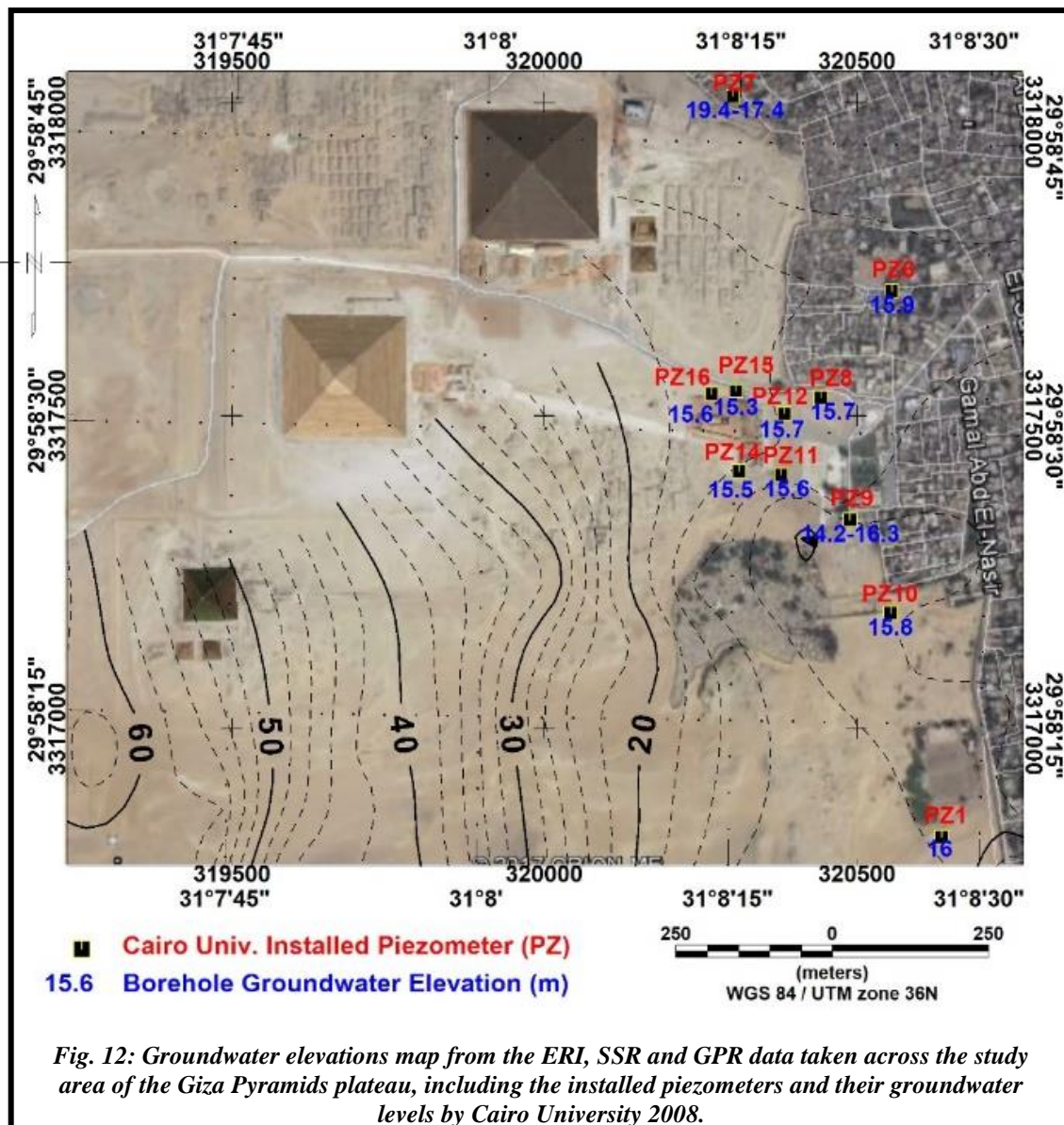
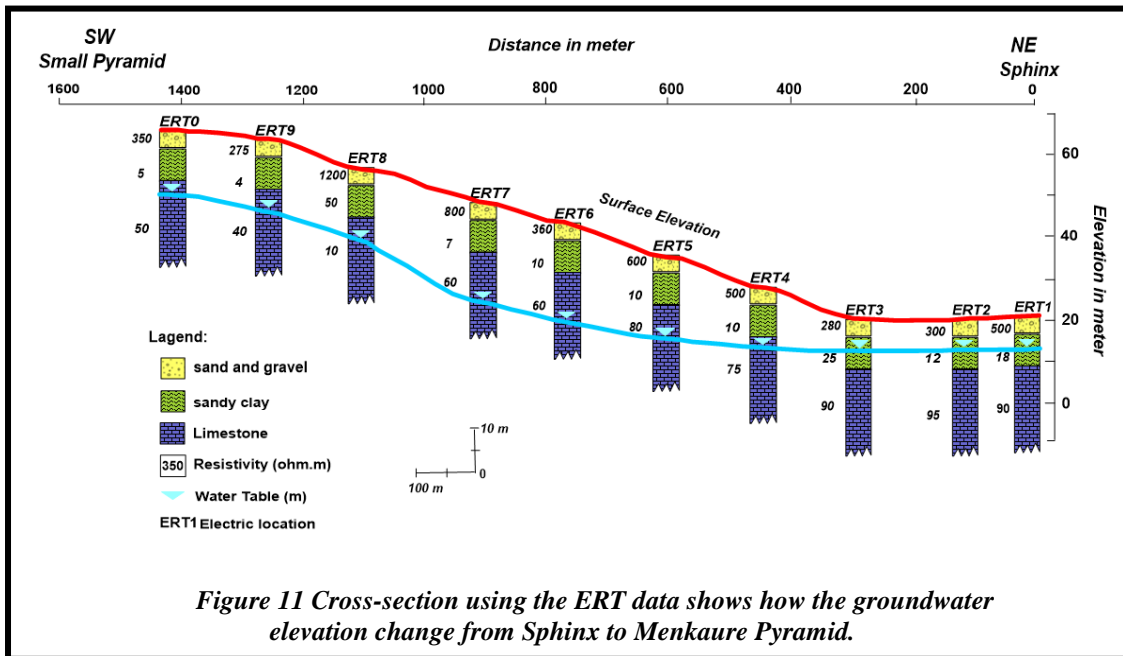
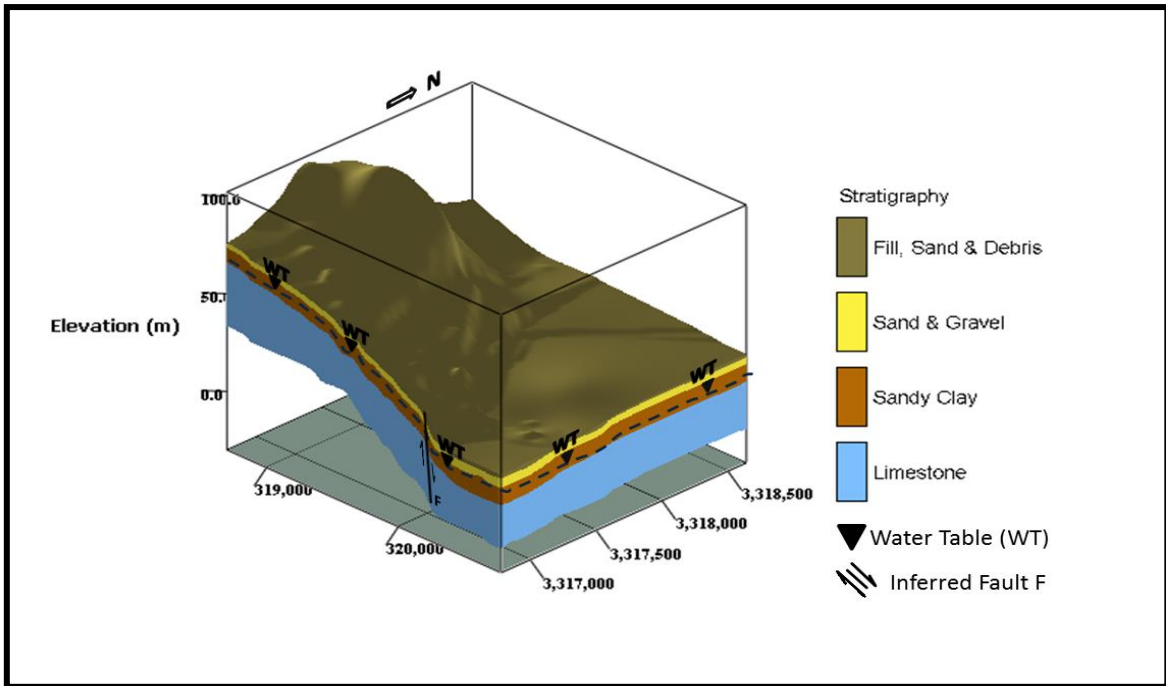


Fig. 10. ERT, SSR and GPR profiles in Cause way to Menkaure Pyramid.

Fig. 9. ERT, SSR and GPR profiles in Valley Temple of Menkaure.





*Fig. 13: 3D model of the Giza Pyramids Plateau, illustrating the groundwater table.*

**Authors' response to the Associate Editor comment on the paper entitled "Shallow Geophysical Techniques to Investigate the Groundwater Table at the Giza Pyramids Area, Giza, Egypt" gi-2017-48**

**Authors: S. M. Sharafeldin, K. S. Essa, M. A. S. Youssef, H. Karsli, Z. E. Diab, and N. Sayil**

We would like to thank Prof. Jothiram Vivekanandan, Chief-Executive Editor, Prof. Andrea Benedetto, the Associate Editor, and the reviewer for their constructive comments for improving our manuscript.

**Replies to the comments of the reviewer**

**Comment #1:-**

**"Authors present a case study dealing with a multi sensor approach in the assessment of the water table level in the Giza Plateau. The field data were collected by using 3 different geophysical techniques: ERI, SSR, GPR. Field setups and measurements procedures are quite well described".**

**Reply:**

Thank you very much for your valuable and helpful comments. We have gone through the manuscript taken into your considerations (corrected, modified and added the missing figures).

**Comment #2:-**

**"I suggest the authors to introduce additional information about the gauges calibration."**

**Reply:**

We have done this in the text in GPR by measuring the velocity by using Unshielded Pulsed-Ekho GPR as stated in the text.

**Comment #3:-**

**"The data processing and analysis is performed through existing software. It is not clear in the text the use of the boreholes data. The paper does not present novel tools or analysis techniques; furthermore the integration of data, collected through different instruments, is quite common. Despite this, the study can be interesting for the specific investigation site and for a cost-effective planning of future measurement campaigns."**

**Reply:**

We have added a new table to compare the WT elevation results between piezometers and geophysical surveys results.

**Comment #4:-**

**"A more interesting data presentation could be obtained by introducing the uncertainty in the analysis."**

**Reply:**

This was done by calculating the RMS errors between measured and calculated arrival time. Also, in the models of ERI, the RMS illustrated on the figures.

**Comment #5:-**

**"The text is generally well written, but sometimes it is redundant. As noticed by the SC1, figures are not in the pdf."**

**Reply:**

Thank you very much for your valuable and helpful comments. We have modified the text to avoid the redundant sentences. Also, we have added the missing Figures.

**Thank you**